Effects of pH and substituted 1,2-dihydroxybenzenes on the reaction pathway of Fenton-like systems

Pablo Salgado[a,c], Victoria Melin[c], Milenka Albornoz[c], Héctor Mansilla[b], Gladys Vidal[a], David Contreras[b,c,*]

[a] Grupo de Ingeniería y Biotecnología Ambiental, Facultad de Ciencias Ambientales y Centro EULA-Chile, Universidad de Concepción, Casilla 160-C, Concepción, Chile
[b] Facultad de Ciencias Químicas, Universidad de Concepción, Casilla 160-C, Concepción, Chile
[c] Centro de Biotecnología, Universidad de Concepción, Concepción, Chile

A B S T R A C T

The Fenton reaction is a redox cycle in which iron reacts with H_2O_2 to produce several reactive species, such as hydroxyl radicals ($\cdot OH$), perhydroxyl radicals ($\cdot OOH$), ferryl ions (Fe(IV)) and singlet oxygen ($^1O_2$). The type and amount of reactive species produced by this redox system can change depending on the reaction conditions. For example, ligands, such as 1,2-dihydroxybenzene (1,2-DHB), can promote the Fenton reaction primarily by promoting the availability of Fe(II) to react with H_2O_2.

Previously, our group determined that the presence of a substituent at the 4-position of 1,2-DHB can change the mechanism, producing $\cdot OH$ radicals by these systems at pH 3.4. In the present work, the effect of various substituents at the 4-position of 1,2-DHB was evaluated at different pH values ranging from 1 to 11. The iron reduction availability and the speciation of the iron complexes with the 1,2-DHBs were related to the reactivity of each system. The reactivity was evaluated by measuring the oxidation of several dyes and the production of different reactive species. It was concluded that 1,2-DHB can increase the reactivity of the Fenton systems at pH values between 1 and 7. However, the reactive species produced at each pH did not change. Under acidic pH conditions, $\cdot OH$ radicals were still the main reactive species produced, and under neutral pH conditions, Fe(IV) was responsible for the oxidizing ability of the Fenton systems.

1. Introduction

The oxidative ability of a mixture of Fe(II) and H_2O_2 was discovered in 1894 by H.J.H. Fenton [1]. Since then, several studies have been performed to propose different mechanisms and applications for Fenton reagents.

The most accepted mechanism for the Fenton reaction was proposed by Haber and Weiss [2]. In this mechanism, Fe(II) reduces H_2O_2 to produce hydroxyl radicals ($\cdot OH$) (1). Fe(III) produced by the Fenton reaction can also oxidize H_2O_2 to form perhydroxyl radicals ($HO_2\cdot$) (2). This reaction is known as a Fenton-like reaction.

$$Fe^{2+} + H_2O_2 \rightarrow Fe^{3+} + \cdot OH + OH^- \tag{1}$$

$$Fe^{3+} + H_2O_2 \rightarrow Fe^{2+} + HO_2\cdot + H^+ \tag{2}$$
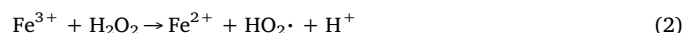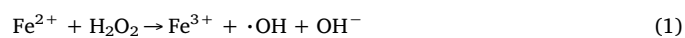
The reactive species produced in Fenton and Fenton-like reactions can participate in parallel reactions to produce singlet oxygen ($^1O_2$) [3] or hypervalent iron species, such as ferryl ions (Fe(IV) or FeO^{2+}) [[4–12],5]. The primarily produced species ($\cdot OH$, $HO_2\cdot$, $^1O_2$ or Fe(IV)) depends of the reaction conditions [4–12]. Several researchers have proposed the importance of the pH for changing the coordination sphere around iron. In addition, it is suggested that analytical methods used to evaluate Fenton systems are important to observe different oxidizing species.

Some ligands on iron can promote the production of reactive species in Fenton systems. Among these ligands, 1,2-dihydroxybenzene (1,2-DHB) is highlighted because of its role in oxidative stress in cells, diseases (such as cancer, Alzheimer's or Parkinson's disease) and advanced oxidation processes (AOPs) for water remediation.

1,2-DHB can form different complexes with iron, where the iron:ligand ratio is pH dependent. In general, only the monocomplex (Fe^{III}-catecholate) can reduce Fe(III) and improve the availability of Fe(II) to produce $\cdot OH$ radicals. However, the mechanism to increase radical production changes depending on the substituent at the 4-position. For substituents with electron-donating groups (EDGs), which have positive Hammett constants (σ), the increase of the $\cdot OH$ radical production depends only on the Fe(III) reduction ability. On the other hand, for substituents with electron-withdrawing groups (EWGs),

which have negative σ values, iron reacts with hydrogen peroxide while the metal is still in the monocomplex form. Thus, the electron is transferred from 1,2-DHB to H_2O_2 through iron with subsequent production of ·OH radicals [13]. Since these results were obtained at a pH of 3.0, the effect of the pH and thus different species on the reactivity of the Fenton-like system driven by 1,2-DHB with different substituents is unknown. The changes in the coordination sphere of Fe(III) due to changes in the pH value could be related to the reactivity of the system over a substrate and the production of reactive species.

In this paper, the indirect determination of reactive species is performed and is related to the reactivity of the system over substrates. Different speciations of the iron complexes were evaluated by changing the pH and the substituents on 1,2-DHB.

2. Experimental

2.1. Chemicals

Ferric nitrate ($Fe(NO_3)_3$), potassium fluoride (KF), ferrozine, 2,3-diaminephenazine (DAPN), *o*-phenylendiamine (OPDA), 2-propanol, sodium azide, dimethylsulfoxide (DMSO), [9-(2-carboxyphenyl)-6-diethylamino-3-xanthenylidene]-diethylammonium chloride (rhodamine B, RhB), 2,7-naphthalenedisulfonic acid, 4-amino-5-hydroxy-3,6-*bis* [(E)-[4-[[2-(sulfooxy)ethyl]sulfonyl]phenyl]azo]-tetrasodium salt (reactive black 5, RB5), 4-[4-(dimethylamino)phenylazo]benzenesulfonic acid sodium salt (methyl orange, MO), 3,3′-(3,3′-dimethoxy-4,4′-biphenylene)bis[2-(4-nitrophenyl)-5-phenyl-2H-tetrazolium chloride] (nitroblue tetrazolium, NBT), 2,6-dichloroindophenol (DCIP), catechol, 3,4-dihydroxybenzonitrile, 4-*tert*-buthylcatechol and 4-methylcatechol were purchased from Sigma-Aldrich. 3,4-Dihydroxybenzoic acid, hydrogen peroxide (H_2O_2, 30% w/w), NaOH, potassium nitrate (KNO_3) and ferrous sulfate ($FeSO_4$) were purchased from Merck.

All reagents were used without additional purification.

2.2. General procedures

All solutions were prepared in the dark under an argon atmosphere. The ionic strengths of all the solutions were adjusted to $0.10\,mol\,L^{-1}$ with KNO_3. All experiments were performed at 20 ± 0.1 °C in triplicate (n = 3).

The pH of each solution was adjusted prior to the experiments using a Thermo Scientific Orion 3-Star pH meter. The pH values between 1.0 and 5.0 were adjusted with HNO_3. For pH values between 6 and 11, non-coordinating buffers of tertiary amines were used. Specifically, 4-morpholineethanesulfonic acid (MES, pKa = 6.1), 1,4-piperazinediethanesulfonic acid (PIPES, pKa = 6.8), 4-(2-hydroxyethyl)-1-piperazinepropanesulfonic acid (EPPS, pKa = 8.0), 2-(cyclohexylamino)ethanesulfonic acid (CHES, pKa = 9.3) and 3-(cyclohexylamino)-1-propanesulfonic acid (CAPS, pKa = 10.4) were used as buffers.

A UV–vis diode array spectrophotometer (Agilent 8453) was used for all the spectrophotometric measurements.

2.3. Speciation and composition of the iron complexes

To understand the effect of 1,2-DHBs on the Fenton-like systems, the types of complexes formed at different pH values were determined. First, the optimum pH for each possible complex was determined spectrophotometrically. Then, the composition of each complex was determined by the method of continuous variations [14,15]. The pH of each solution was adjusted with the corresponding buffers. The concentrations of the Fe(III) and 1,2-DHB solutions ranged from 0 to $6.0 \times 10^{-4}\,mol\,L^{-1}$ and from 6.0×10^{-4} to $0\,mol\,L^{-1}$, respectively, maintaining a total concentration ([Fe(III)] + [1,2-DHB]) of $6.0 \times 10^{-4}\,mol\,L^{-1}$ in each measurement. To measure the spectra at acidic pH values, a stopped-flow spectrophotometric determination

method was used. At neutral and basic pH values, the reagents were mixed, and the spectra were measured after 1 h in a quartz cuvette.

The pH range over which each complex formed a predominant species was determined with isosbestic points. Two maximum absorbances at neighboring wavelengths on both sides of an isosbestic point were considered [16]. From the plot of this absorbance as a function of pH, an intercept that indicated the transition pH between the complexes was found.

2.4. Reduction of Fe(III)

The reduction of Fe(III) by different 1,2-DHBs was determined by quantifying the Fe(II) produced at different reaction times at pH values between 1.0 and 11.0. The formed Fe(II) was detected as a colored complex with ferrozine (λ_{max} = 562 nm) [17].

From a reactor containing $5.0 \times 10^{-4}\,mol\,L^{-1}$ Fe(III) and $1.0 \times 10^{-4}\,mol\,L^{-1}$ 1,2-DHB, an aliquot was taken at different reaction times, and this aliquot was added to a cuvette containing $0.20\,mol\,L^{-1}$ KF and $5.0 \times 10^{-3}\,mol\,L^{-1}$ ferrozine at pH 5.5. The concentration of the ferrozine-Fe(II) complex was determined from a calibration curve constructed at pH 5.5.

Each plot was fit with pseudo-first-order kinetics according to Eq. (3), and from this, the rate constant of Fe(III) reduction (k_{red}) was calculated.

$$\ln[Fe(II)]_t = k_{red}t + \ln[Fe(II)]_0 \tag{3}$$

2.5. Determination of ·OH radicals

The ·OH radicals were determined at different pH values by an indirect method based on the reaction of these radicals with OPDA. This reaction produced DAPN, which absorbs at 453 nm [18,19]. The final concentrations in the systems were $2.0 \times 10^{-5}\,mol\,L^{-1}$ Fe(III), $2.0 \times 10^{-5}\,mol\,L^{-1}$ H_2O_2, $1.0 \times 10^{-6}\,mol\,L^{-1}$ 1,2-DHB and $5 \times 10^{-4}\,mol\,L^{-1}$ OPDA. Calibration curves of DAPN were generated at each pH studied to obtain the DAPN concentrations.

The plot of the DAPN concentration versus time at each pH value was fit by pseudo-first-order kinetics according Eq. (4), which was used to determine the rate constant of DAPN production (k_{DAPN}).

$$\ln[DAPN]_t = k_{DAPN}t + \ln[DAPN]_0 \tag{4}$$

2.6. Determination of $O_2\cdot^-/HO_2\cdot$ radicals

To determine the $HO_2\cdot$ radicals, three different methods were used: the reduction of NBD-Cl to give a colored product with λ_{max} = 470 nm [20], the formation of two colored species (λ_{max} = 405 nm and λ_{max} = 530 nm) from the reduction of NBT [21] and the reduction of *p*-benzoquinone to produce a colored SQ· with λ_{max} = 430 nm [22,23]. The final concentrations were $2.0 \times 10^{-5}\,mol\,L^{-1}$ Fe(III), $2.0 \times 10^{-5}\,mol\,L^{-1}$ H_2O_2, $1.0 \times 10^{-6}\,mol\,L^{-1}$ 1,2-DHB and $5.0 \times 10^{-4}\,mol\,L^{-1}$ NBD-Cl, NBT and *p*-benzoquinone. NBT was prepared in an aqueous solution, while NBD-Cl and *p*-benzoquinone were prepared in acetonitrile.

2.7. Oxidation of the dyes

To evaluate the oxidizing ability of the Fenton-like systems driven by 1,2-DHBs with different substituents and at different pH values, the degradation percentages of the dyes were determined after 1 h of reaction. The dyes used were RB5 (λ_{max} = 598 nm), which corresponds to ferryl production [5]; RhB (λ_{max} = 564 nm), which is primarily oxidized by ·OH radicals [24]; DCIP (λ_{max} = 600 nm), which is used as an indicator of $O_2\cdot^-$ radical production [22]; and MO (λ_{max} = 508 nm), which is widely used as a model compound for degradation. The final concentrations in each system were $2.0 \times 10^{-5}\,mol\,L^{-1}$ Fe(III),

2.0×10^{-5} mol L^{-1} H$_2$O$_2$, $1.0 \times 10^{-}$ mol L^{-1} 1,2-DHB and 1.0×10^{-5} mol L^{-1}dyes. Scavengers were employed to identify differences in the reactive species produced in the studied systems. The scavengers used were 2-propanol (highly selective for ·OH radicals) [25], sodium azide (selective for ^{1}O$_2$) [26] and DMSO (selective for ·OH radicals and ferryl ions) [[24],27]. For these experiments, the scavenger concentration was 5.0×10^{-3} mol L^{-1}.

2.8. Stability of the Fe(III) biscomplex in the presence of H$_2$O$_2$

To evaluate the possible interaction between H$_2$O$_2$ and iron at pH 7.0, biscomplexes were prepared at this pH by mixing 2.0×10^{-5} mol L^{-1} Fe(III) and 2.0×10^{-4} mol L^{-1} 1,2-DHB. After 1 h, the solution with the biscomplex was mixed with 2.0×10^{-3} mol L^{-1} H$_2$O$_2$ using the UV–vis diode array spectrophotometer (Agilent 8453) coupled with a stopped-flow system (Applied Photophysics RX2000). The change in the spectrophotometric signal of the biscomplex was followed at the maximum absorption wavelength of each biscomplex.

2.9. Substituent effects

The Hammett equation (Eq. (5)) was used to study the effects of the substituents on 1,2-DHB in the reactivity of the studied systems. In this equation, k$_{obs}$ is the rate constant for substituent X, and k$^{\circ}_{obs}$ is the rate constant when X = H.

$$\log\frac{k_{obs}}{k^{\circ}_{obs}} = \sigma\rho \tag{5}$$

The reaction constant (ρ), obtained from the slope of the plot constructed with the Hammett equation, provides a measure of the reaction sensitivity to the electronic effects of the substituents. Considering that 1,2-DHB has two hydroxyl groups and one substituent, in this work, the effect of the substituent was evaluated by the sum of the values of σ$_m$ and σ$_p$ (Σσ) [28,29]. Table 1 shows the studied 1,2-DHBs, their abbreviations, the Hammett parameters (σ$_m$ and σ$_p$) and Σσ.

2.10. Statistical analyses

To determine the significance of the parameters analyzed in this study, ANOVA and post-test (Tukey) calculations were performed to compare the differences between means. These statistical analyses were performed using GraphPad InStat 3 (GraphPad Software, Inc.) software.

3. Results and discussion

3.1. Composition of the ferric complexes as a function of pH

To understand the effect of 1,2-DHB on the Fenton and Fenton-like systems at different pH values, the speciation of each iron complex was determined. The UV–vis absorption spectra were recorded at pH values from 1.0 to 11.0 (Fig. 1). Intense ligand-to-metal charge-transfer (LMCT) bands were detected over the entire pH range. All the 1,2-DHBs show a shift of the charge-transfer band from a wavelength near 500 nm up to 700 nm by decreasing the pH due to a change in the type of complex present in solution.

Table 1
Studied 1,2-DHBs and their Hammett parameters [30].

Abbreviation	1,2-Dihydroxybenzene	σ$_m$	σ$_p$	Σσ (= σ$_m$ + σ$_p$)
4-TC	4-*Tert*-butylcatechol	−0.10	−0.20	−0.30
4-MC	4-Methylcatechol	−0.07	−0.15	−0.22
CAT	Catechol	0.00	0.00	0.00
4-COOH	3,4-Dihydroxybenzoic acid	0.37	0.45	0.82
4-CN	3,4-Dihydroxybenzonitrile	0.56	0.66	1.22

By analyzing the UV–vis spectra at different pH values (Figs. S1 and S2), the coordination number of each complex in solution was determined. The absorption band near 500 nm corresponds to the triscomplex formed only at basic pH. At near-neutral pH, primarily the biscomplex with an absorbance between 550 and 600 nm is formed, and at acidic pH, the monocomplex with an absorbance above 700 nm is formed (Fig. 2). These results are in accordance with previous reports by other researchers on the study of other catechol complexes [31–33].

A specific pH range was established in which a predominant type of complex was formed (Figs. S3 and S4), highlighting that the pH range for the monocomplex formation is dependent on the substituent on 1,2-DHB (Table 2). For the monocomplex of 1,2-DHB with an EWG, the maximum pH is 4.3, while for the monocomplex of 1,2-DHB with an EDG, the maximum pH is almost 5.3. This finding can be explained by considering the different acidities of the hydroxyl groups on 1,2-DHB. The reported pKa values of the hydroxyl groups on the 1,2-DHB with an EWG are lower than the corresponding pKa values for the 1,2-DHB with an EDG [34–37] (Table S1). Thus, the further deprotonation of 1,2-DHB with an EWG at a pH near 5.0 promotes the formation of a biscomplex over a monocomplex.

Note that the monocomplex has been associated with the complex formed by Fe(III)-catechol [31,32,38,39] by some authors and with the Fe(II)-semiquinone complex by others researchers [40,41]. This controversy remains due to the difficulty in studying the monocomplex because of its high instability.

3.2. Fe(III) reduction by 1,2-DHB

The ability of the 1,2-DHBs with different substituents to reduce Fe(III) was determined at pH values between 1.0 and 11.0. Fe(II) obtained from the reduction of Fe(III) by 1,2-DHB was quantified after 1 h of reaction (Fig. 3). All the 1,2-DHBs studied showed Fe(III) reduction only under acidic pH conditions (1.0, 3.0 and 5.0). At pH values of 7.0, 9.0 and 11.0, the amount of Fe(II) was under the detection limit (8×10^{-7} mol L^{-1}). This observation is in accordance with previous reports on catecholamines and other DHBs and is related to the presence of monocomplexes [17,42,43]. Otherwise, under neutral and basic pH conditions, under detection limit amount of Fe(II) was associated with the formation of bis- and triscomplexes, thus indicating a lack of Fe(III) reduction.

To analyze the substituent effects on the reduction of Fe(III) by the 1,2-DHBs, the rate constants of Fe(III) reduction (k$_{red}$) were determined (Table S2) and were related to Σσ (Fig. 4). A linear dependence between these two parameters was observed. The results show a dependence of the k$_{red}$ value on the substituent on the 1,2-DHB. The 1,2-DHBs with EDGs reduced Fe(III) at a higher rate than the 1,2-DHBs with EWGs. The slopes (ρ) obtained are pH dependent, displaying values of -0.35 ± 0.02 at pH 1.0 (r = 0.995), -0.39 ± 0.02 at pH 3.0 (r = 0.996) and -0.65 ± 0.03 at pH 5.0 (r = 0.995). Under these reaction conditions, all the ρ values were negative, indicating a decrease in the electron density at the reaction center in the rate-limiting step of the reaction, which is related to electron transfer from the ligand to the metal to produce Fe(II). For the value of ρ, there was no significant difference between pH 1.0 and 3.0, but this value was considerably lower in magnitude than the ρ at pH 5.0. The high ρ value at pH 5.0 is related to the change in the proportion of species present in solution. At pH 5.0, the monocomplex is the main species in solution for systems with a catechol or 1,2-DHB with an EDG. However, at pH 5.0, systems with a 1,2-DHB with an EWG mainly present biscomplexes, which do not reduce Fe(III). Therefore, the portion of the monocomplex in solution is low; consequently, the k$_{red}$ value is greatly diminished. Thus, the difference in the k$_{red}$ values between 1,2-DHB with an EWG and 1,2-DHB with an EDG increases, which promotes an increase in the magnitude of ρ.
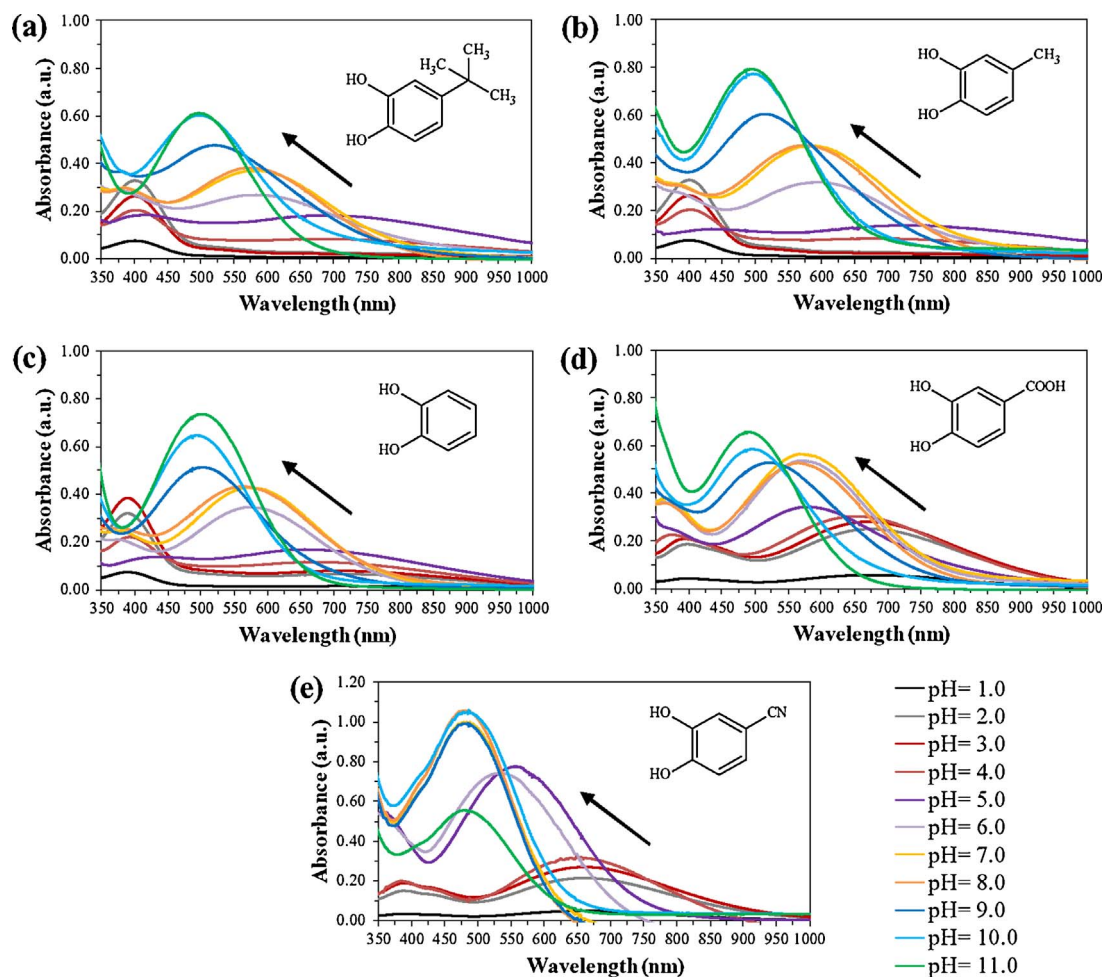
Fig. 1. UV–vis spectra of the iron complexes with (a) 4-*tert*-butylcatechol, (b) 4-methylcatechol, (c) catechol, (d) 3,4-dihydroxybenzoic acid and (e) 3,4-dihydroxybenzonitrile at different pH values. The final concentrations were $1.0 \times 10^{-4}\,\mathrm{mol\,L^{-1}}$ Fe(III) and $1.0 \times 10^{-2}\,\mathrm{mol\,L^{-1}}$ 1,2-DHB. The arrows indicate the direction of increasing pH from 1.0 to 11.0.
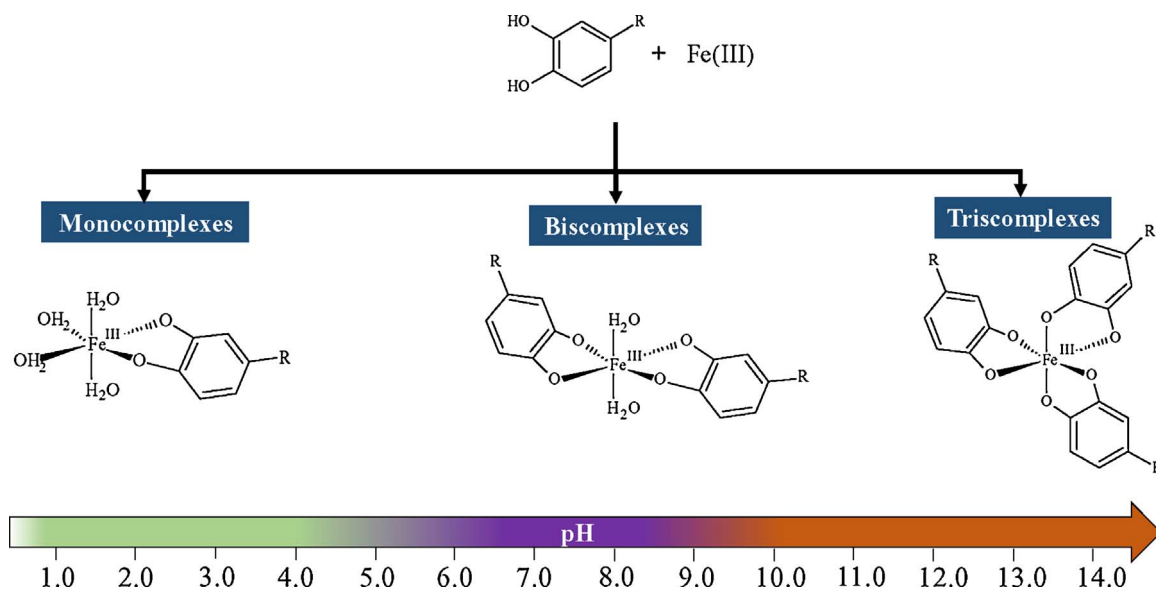

Fig. 2. Iron complexes with 1,2-dihydroxybenzenes as a function of pH.

Table 2
The pH ranges of the monocomplexes, biscomplexes and triscomplexes of Fe(III) with 1,2-dihydroxybenzenes.

1,2-Dihydroxybenzene	pH range		
	Monocomplex	Biscomplex	Triscomplex
4-*Tert*-butylcatechol	1.0–5.19	5.19–8.62	8.62–11.0
4-Methylcatechol	1.0–5.12	5.12–8.46	8.46–11.0
Catechol	1.0–5.08	5.08–8.32	8.32–11.0
3,4-Dihydroxybenzoic acid	1.0–4.28	4.28–8.78	8.78–11.0
3,4-Dihydroxybenzonitrile	1.0–4.19	4.19–6.13	6.13–11.0

3.3. Production of oxidant species in the Fenton and Fenton-like systems driven by 1,2-DHB

3.3.1. Determination of ·OH radicals

The production of ·OH radicals was studied between the pH values of 1.0 and 11.0 using the reaction of this radical with OPDA (colorless) to give DAPN (colored) as a product. This method has the advantages of easy implementation and cost-effectiveness. In addition, this method has been compared with analyses performed by electronic paramagnetic resonance spectroscopy, producing results that are consistent with those obtained by the reaction of OPDA [44,45]. In addition, the product formed by this method is stable, and this compound does not react with H_2O_2 as the DMPO-OH adduct [46,47].

From the DAPN production kinetics (Fig. S5), a considerable production of this compound was observed in all the studied systems at a
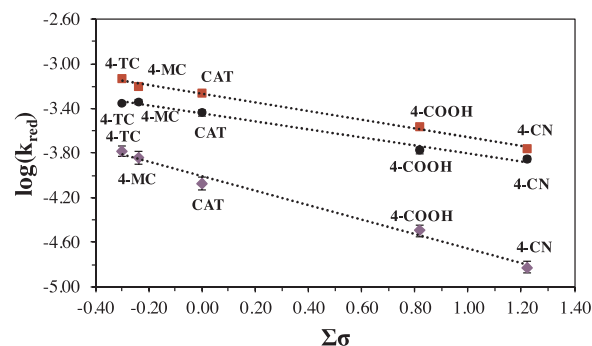

Fig. 4. Relationship between $log(k_{red})$ and the Hammett parameter for each 1,2-DHB used at different pH values. Black circle: pH 1.0; red squares: pH 3.0; purple rhombs: pH 5.0. (For interpretation of the references to color in this figure legend, the reader is referred to the web version of this article.)

pH of 5.0 or lower. Higher concentrations of DAPN were produced at a pH of 3.0. At a pH above 5.0, no significant production of DAPN was detected. These trends of DAPN production at different pH values show that the production of ·OH radicals is independent of the substituent on the 1,2-DHB. This reactivity is primarily related to the speciation of the iron complex with 1,2-DHB, which was discussed in previous works [17,42,43] and was related to the availability of Fe(II) to react with H_2O_2.

The rate constants for the production of DAPN (k_{DAPN}) were obtained from the kinetics of each Fenton-like system driven by 1,2-DHB
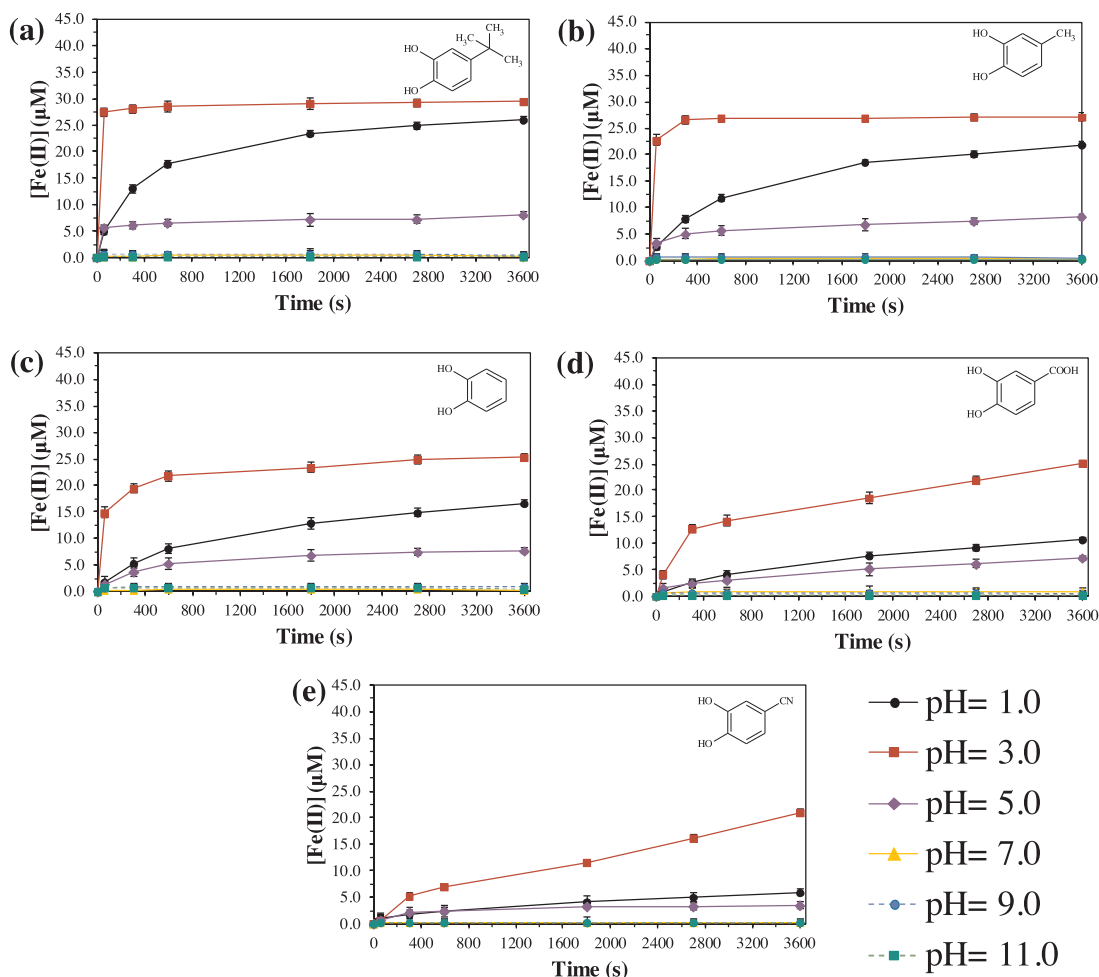

Fig. 3. Kinetic profiles obtained for Fe(III) reduction by a) 4-*tert*-butylcatechol, b) 4-methylcatechol, c) catechol, d) 3,4-dihydroxybenzoic acid and e) 3,4-dihydroxybenzonitrile. (For interpretation of the references to color in this figure legend, the reader is referred to the web version of this article.)
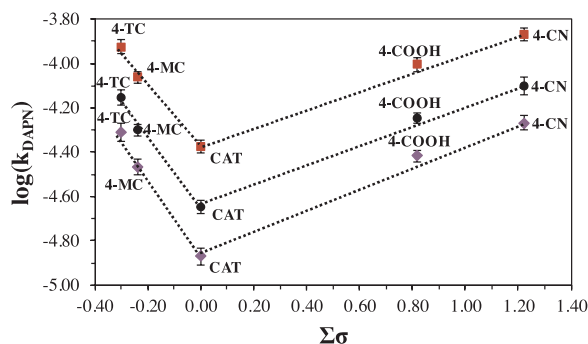
Fig. 5. Relationship between the log(k_{DAPN}) obtained from the Fenton and Fenton-like systems driven by 1,2-DHBs and the Hammett parameters at pH values of 1.0 (black circles), 3.0 (red squares) and 5.0 (purple rhombs). (For interpretation of the references to color in this figure legend, the reader is referred to the web version of this article.)

(Table S3). The k_{DAPN} value was related to the Hammett parameter ($\Sigma\sigma$) to obtain information about the substituent effects on the production of ·OH radicals (Fig. 5).

The trends were similar over the pH range in which a significant production of DAPN could be detected. With substituents that possessed a high ability to donate or remove electron density, higher rates of DAPN production were observed. The minimum rate was observed for the Fenton-like system driven by catechol. Thus, the values of ρ for the Fenton-like systems driven by 1,2-DHB with EDGs were negative, and for Fenton-like systems driven by 1,2-DHBs with EWGs, the ρ values were positive. This difference of ρ indicates that the mechanism to produce ·OH radicals, which formed DAPN, at an acidic pH is dependent on the substituent on the 1,2-DHB.

The pH range in which ·OH radical production was observed was the same range observed for the reduction of Fe(III) by 1,2-DHB. However, only the k_{DAPN} values of the Fenton-like systems driven by 1,2-DHBs with EDGs were directly related to the k_{red} values (Fig. 6). The Fenton-like systems driven by 1,2-DHBs with EWGs produced ·OH radicals by another mechanism involving a peroxocomplex of iron with 1,2-DHB, as previously discussed in another work by our group [13].

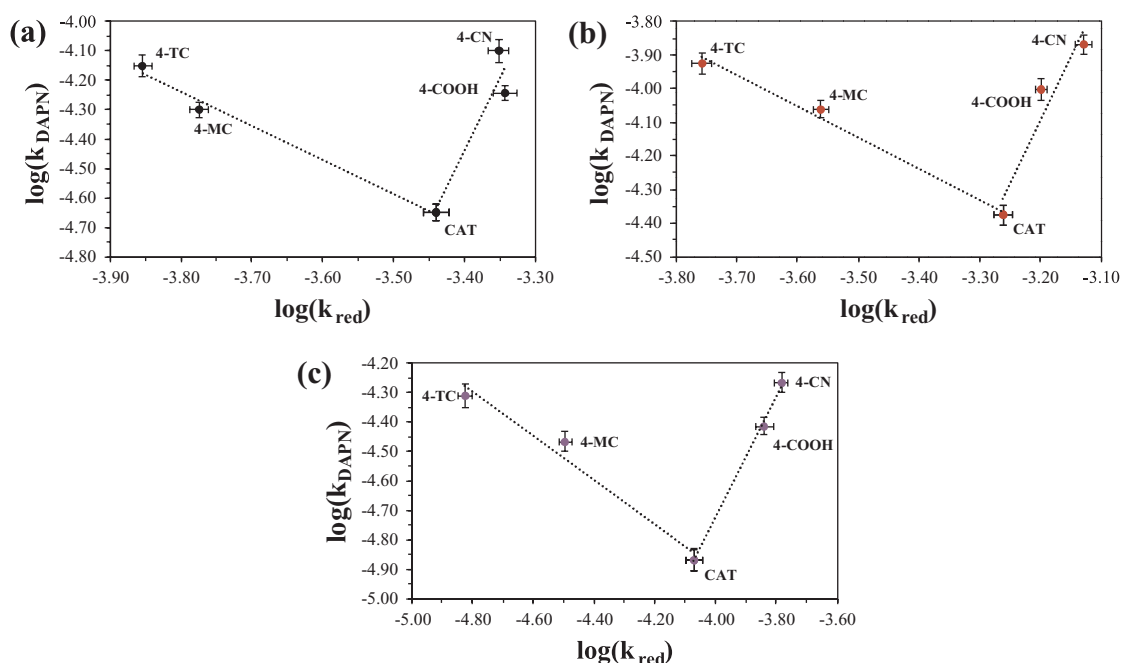### 3.3.2. Determination of $O_2\cdot^-$ or $HO_2\cdot$

Neither $O_2\cdot^-$ nor $HO_2\cdot$ was detected in the studied systems employing the three different methods used to quantify these species.

3.4. Effect on the oxidation of the dyes

To evaluate the oxidizing ability of the Fenton-like systems driven by the different 1,2-DHBs at different pH values, dyes were oxidized over 1 h at pH values between 1.0 and 11. The dyes employed were primarily selected because of their reactive specificity. These dyes were RB5, RhB, DCIP and MO, and the corresponding structures are shown in Fig. S6.

For RB5, RhB and MO, considerable oxidation was observed through a significant decrease in the spectrophotometric signals (Fig. 7). In contrast, DCIP showed no significant discoloration after 1 h of reaction. DCIP is used to measure $O_2\cdot^-/HO_2\cdot$ radical production in biological systems [22], and this lack of oxidation is consistent with the undetected concentration of $O_2\cdot^-/HO_2\cdot$ radicals in the studied systems.

From Fig. 7, similar trends of the degradations of MO and RhB are observed. These dyes were degraded by the Fenton-like systems only under acidic pH conditions. The presence of 1,2-DHB increased the oxidation ability in all the systems. Higher percentages of oxidation were reached at a pH of 3.0, which corresponds with the maximum Fe(III) reduction and DAPN production. The RB5 oxidation was significant over the entire pH range studied. 1,2-DHB promoted the oxidation of this dye only at pH values of 1.0, 3.0 and 7.0. This difference in the dye oxidation trends could be related to the reactive species responsible for the oxidation. To evaluate this possibility, the same reactions were performed in the presence of different scavengers. Azide, 2-propanol, and DMSO were used. Azide is a scavenger of $^1O_2$ [26], 2-propanol is a specific scavenger of ·OH radicals [25], and DMSO is a scavenger of ·OH radicals and ferryl species [4,27]. The presence of azide in the reaction systems resulted in no significant changes in the percentages of oxidation compared with systems without scavengers (Fig. S7). When 2-propanol was included in the reaction systems, the oxidation of MO and RhB was not significant over the entire pH range studied. On the other hand, the oxidation of RB5 was only significantly decreased at pH values below 5.0. At pH 7.0, only the oxidation of RB5 by the Fenton-like system without 1,2-DHB was significantly affected. DMSO prevented
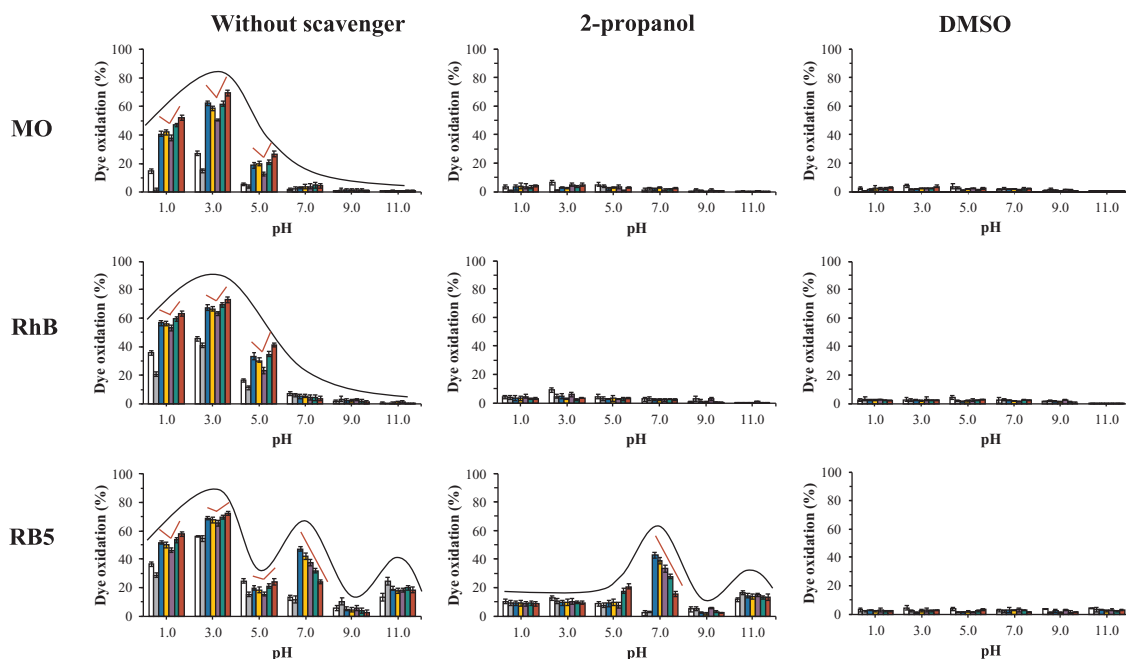

Fig. 6. Relationship between Fe(III) reduction (k_{red}) and the production of ·OH radicals (k_{DAPN}) in the Fenton-like systems driven by 1,2-DHBs at pH values of (a) 1.0, (b) 3.0 and (c) 5.0.

Fig. 7. Percentages of dye oxidation by the Fenton-like systems driven by 1,2-DHB. White bar: Fenton systems without 1,2-DHB; gray bar: Fenton-like systems without 1,2-DHB; blue bar: Fenton-like systems with 4-*tert*-butylcatechol; yellow bar: Fenton-like systems with 4-methylcatechol; purple bar: Fenton-like systems with catechol; green bar: Fenton-like systems with 3,4-dihydroxybenzoic acid; red bar: Fenton-like systems with 3,4-dihydroxybenzonitrile. Black lines highlight the dependence of the dye oxidation over the pH and the red lines highlight the dependence of the dye oxidation over the substituent of the 1,2-DHB.
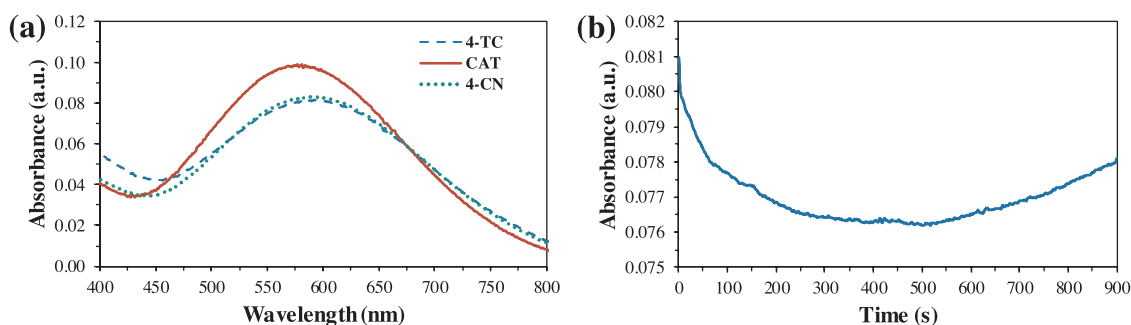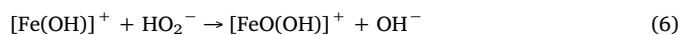

Fig. 8. a) Absorption spectra of the iron biscomplexes with different 1,2-DHBs and b) kinetic profile of the biscomplex between iron and 4-*tert*-butylcatechol in the presence of H_2O_2. (For interpretation of the references to color in this figure legend, the reader is referred to the web version of this article.)

the oxidation of all the dyes at pH values between 1.0 and 11.0.

Together, these results suggest a different oxidant species produced by the Fenton-like systems driven by 1,2-DHB. Under acidic pH conditions, the oxidation of different dyes by these systems primarily occurs via ·OH radicals, and the oxidations are linearly related to the production of DAPN (Fig. S8). At neutral pH, a ferryl species is formed, promoted by the biscomplex present at this pH.

The RB5 oxidation at pH 11 is not promoted by 1,2-DHB because no significant differences were observed between the Fenton or Fenton-like systems without 1,2-DHB and the Fenton-like systems driven by 1,2-DHB. Moreover, 2-propanol did not prevent the oxidation of this dye, indicating that at pH 11.0, the oxidation of RB5 is not responsible for ·OH radical production. The results obtained in the presence of DMSO suggest the participation of hypervalent iron species as ferryl ions. The formation of ferryl species at a strongly basic pH and by a DHB-independent pathway was suggested by Lee et al. [5] and has a possible effect due to the iron and H_2O_2 speciation (Eqs. (6) and (7)).

$$[Fe(OH)]^+ + HO_2^- \rightarrow [FeO(OH)]^+ + OH^- \qquad (6)$$

$$Fe(II) + HO_2^- \rightarrow [FeO]^{2+} + OH^- \qquad (7)$$

3.5. Stability of the Fe(III) biscomplexes in the presence of H_2O_2

The stabilities of the Fe(III) biscomplexes formed with different 1,2-DHBs in the presence of H_2O_2 were analyzed to evaluate whether these complexes participate in the formation of reactive species at pH 7.0. The biscomplexes at pH 7.0 were formed, and after 1 h, an aliquot of H_2O_2 was added. Then, the UV–vis spectra were followed every 0.5 s in a stopped-flow system. The spectrophotometric signals of the Fe(III) biscomplexes at pH 7.0 are shown in Fig. 8a. For simplicity, the figure only shows an example of each type of substituent: *tert*-butylcatechol (4-TC) as an example of an EDG, 3,4-dihydroxybenzonitrile (4-CN) as an EWG and catechol (CAT) for a substituent-free species. All the biscomplexes studied showed a decrease at the corresponding wavelength over the first 300 s, but then, these signals remained nearly unchanged over the next 300 s before starting to increase (Fig. 8b).

From a detailed analysis of the spectrum (Fig. 9), it was observed that the increment of the biscomplex signal was due to the appearance of a species with an absorbance wavelength lower but close to the maximum wavelength of the biscomplex.

It is remarkable that the Fe(III) biscomplexes formed by the 1,2-DHB with EDGs in the presence of H_2O_2 decay faster than those formed by 1,2-DHBs with EWGs (Table S4). The rate constants of these decays
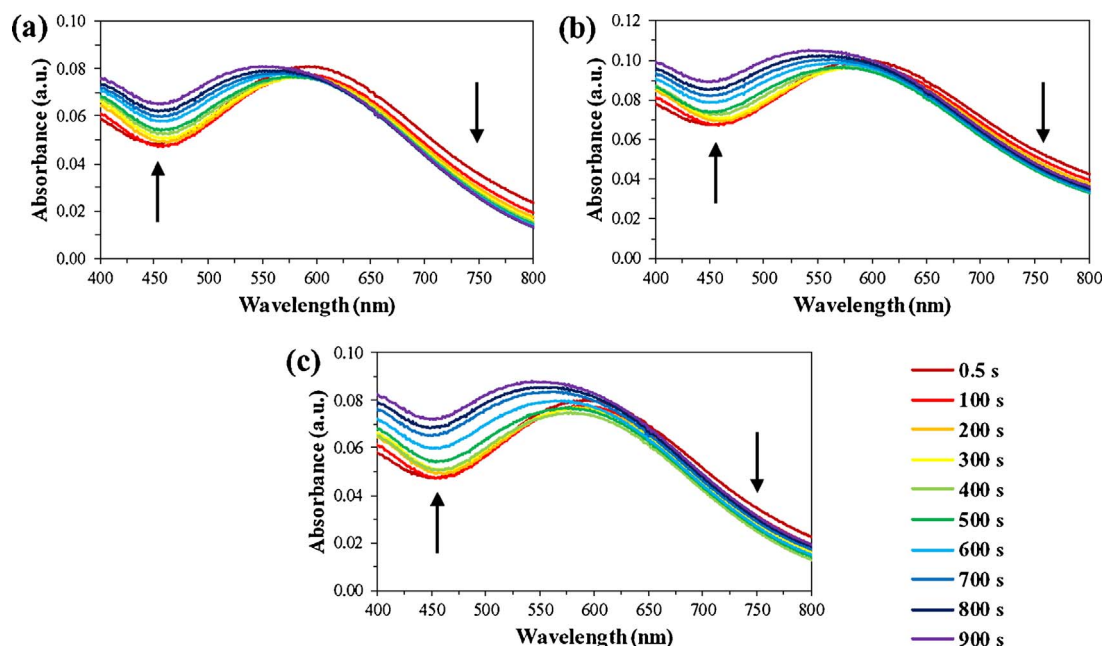
Fig. 9. Absorbance changes of the biscomplexes of iron with 1,2-DHBs for the absorption bands of a) 4-*tert*-butylcatechol, b) catechol and c) 3,4-dihydroxybenzonitrile after adding H_2O_2 to the solutions.
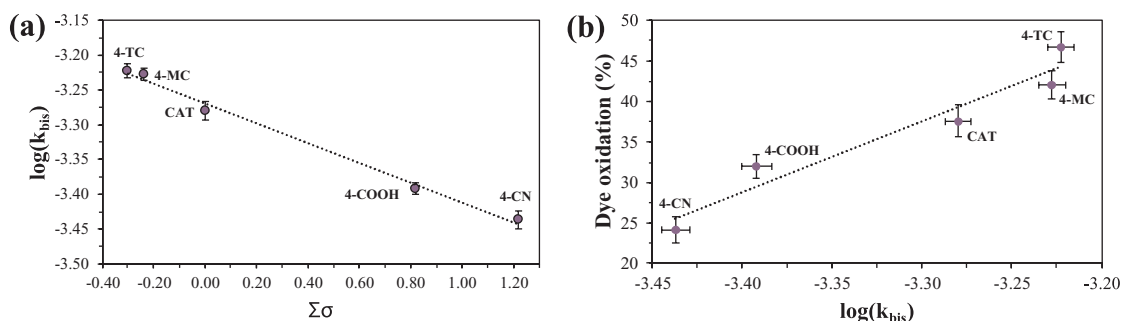

Fig. 10. a) Relationship between the decay constants of the ferric biscomplexes in the presence of H_2O_2 (k_{bis}) with the Hammett constants ($\Sigma\sigma$), and b) the relationship between $log(k_{bis})$ and the percentage of RB5 oxidation.
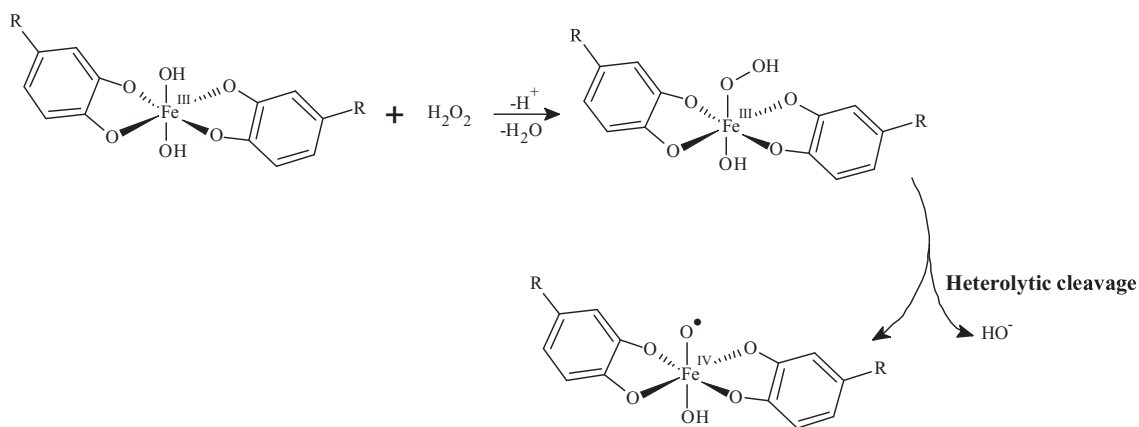

Fig. 11. Pathway proposed for the formation of the Fe(IV) complexes.

(k_{bis}) were linearly related to the Hammett parameters and to the percentages of oxidation of RB5 (Fig. 10a and b, respectively).

Together, these results suggest that the degradation of RB5 was caused by Fe(IV), which could be formed by an interaction between the Fe(III) biscomplex and H_2O_2. The substituent present on the 1,2-DHB changed the rate at which the peroxocomplex was formed, and this directly affected the ability to form Fe(IV). After the inclusion of H_2O_2,

Fe(IV) was formed in the biscomplex by heterolytic cleavage (Fig. 11). Our results are in agreement with those reported by Wang et al. [48]. In their work, the authors propose the formation of peroxocomplexes prior to the formation of hypervalent copper species (Cu(III)) by copper-Fenton systems (Cu(II)/H_2O_2). In addition, Wang observed that the presence of EDGs on the copper ligands promoted the formation of these peroxocomplexes. Malik proposed a similar reaction pathway for

Fe(III) complexes and H_2O_2 [49].

The formation of Fe(IV) in the Fenton-like systems driven by 1,2-DHB only occurs at pH values where the biscomplex is formed because the biscomplex is stable and possesses labile positions for H_2O_2 inclusion. The monocomplex is unstable, thus it cannot promote Fe(IV) formation. The triscomplex is stable but has completely occupied coordination sites; thus, the ligands do not allow interaction with H_2O_2.

4. Conclusions

The types of reactive species produced in Fenton-like systems are pH dependent. The participation of the 1,2-DHB ligands in the coordination sphere increases the amount of reactive species produced. In this way, under acidic pH conditions, mainly ·OH radicals were detected, and under neutral pH conditions, the main species produced was Fe(IV).

The effect of the substituent on the electron density of the 1,2-DHB was related to the mechanism of ·OH radical production at pH values under 5. Additionally, at neutral pH, the relative amount of Fe(IV) was linearly related to the electron density on the ligand, which is determined by the substituent.

Acknowledgements

Appendix A. Supplementary data

Supplementary data associated with this article can be found, in the online version, at https://doi.org/10.1016/j.apcatb.2017.12.035.

References

[1] H.J.H. Fenton, LXXIII.–Oxidation of tartaric acid in presence of iron, J. Chem. Soc. Trans. 65 (1894) 899–910.

[2] F. Haber, J. Weiss, Über die Katalyse des Hydroperoxydes, Naturwissenschaften 20 (1932) 948–950.

[3] I.P. Ivanova, S.V. Trofimova, I.M. Piskarev, N.A. Aristova, O.E. Burhina, O.O. Soshnikova, Mechanism of chemiluminescence in Fenton reaction, J. Biophys. Chem. 3 (2012) 4.

[4] H. Bataineh, O. Pestovsky, A. Bakac, pH-Induced mechanistic changeover from hydroxyl radicals to iron(iv) in the Fenton reaction, Chem. Sci. 3 (2012) 1594–1599.

[5] H. Lee, H.-J. Lee, D.L. Sedlak, C. Lee, pH-Dependent reactivity of oxidants formed by iron and copper-catalyzed decomposition of hydrogen peroxide, Chemosphere 92 (2013) 652–658.

[6] S. Goldstein, D. Meyerstein, G. Czapski, The fenton reagents, Free Radic. Biol. Med. 15 (1993) 435–445.

[7] I. Yamazaki, L.H. Piette, EPR spin-trapping study on the oxidizing species formed in the reaction of the ferrous ion with hydrogen peroxide, J. Am. Chem. Soc. 113 (1991) 7588–7593.

[8] B. Halliwell, J.M.C. Gutteridge, Formation of a thiobarbituric-acid-reactive substance from deoxyribose in the presence of iron salts, FEBS Lett. 128 (1981) 347–352.

[9] M. Strlic, J. Kolar, V.-S. Selih, D. Kocar, B. Pihlar, A comparative study of several transition metals in Fenton-like reaction systems at circum-neutral pH, Acta Chim. Slov. 50 (2003) 619–632.

[10] H.C. Sutton, Formate oxidation induced by a copper peroxo complex produced in Fenton-like reactions, J. Chem. Soc. Faraday Trans. 1: Phys. Chem. Condens. Phases 85 (1989) 883–893.

[11] S.H. Bossmann, E. Oliveros, S. Göb, S. Siegwart, E.P. Dahlen, L. Payawan, M. Straub, M. Wörner, A.M. Braun, New evidence against hydroxyl radicals as reactive intermediates in the thermal and photochemically enhanced Fenton reactions, J. Phys. Chem. A 102 (1998) 5542–5550.

[12] W. Freinbichler, K.F. Tipton, L.D. Corte, W. Linert, Mechanistic aspects of the Fenton reaction under conditions approximated to the extracellular fluid, J. Inorg. Biochem. 103 (2009) 28–34.

[13] P. Salgado, V. Melin, Y. Durán, H. Mansilla, D. Contreras, The reactivity and reaction pathway of Fenton reactions driven by substituted 1,2-dihydroxybenzenes, Environ. Sci. Technol. 51 (7) (2017) 3687–3693.

[14] F.R. Mansour, N.D. Danielson, Ligand exchange spectrophotometric method for the determination of mole ratio in metal complexes, Microchem. J. 103 (2012) 74–78.

[15] P.V. Chalapathi, B. Prathima, Y. Subba Rao, G.N. Ramesh, A. Varada Reddy,

[16] B.A.F. Previdello, F.d. Carvalho, A.L. Tessaro, V. Souza, N. Hioka, O pKa de indicadores ácido-base e os efeitos de sistemas coloidais, Quím. Nova 29 (2006) 600–606.

[17] V. Melin, A. Henríquez, C. Radojkovic, B. Schwederski, W. Kaim, J. Freer, D. Contreras, Reduction reactivity of catecholamines and their ability to promote a Fenton reaction, Inorg. Chim. Acta 453 (2016) 1–7.

[18] Y.F. Fang, A.P. Deng, Y.P. Huang, Determination of hydroxyl radical in Fenton system, Chin. Chem. Lett. 20 (2009) 1235–1240.

[19] K. Toda, T. Tanaka, Y. Tsuda, M. Ban, E.P. Koveke, M. Koinuma, S.-I. Ohira, Sulfurized limonite as material for fast decomposition of organic compounds by heterogeneous Fenton reaction, J. Hazard. Mater. 278 (2014) 426–432.

[20] R.O. Olojo, R.H. Xia, J.J. Abramson, Spectrophotometric and fluorometric assay of superoxide ion using 4-chloro-7-nitrobenzo-2-oxa-1,3-diazole, Anal. Biochem. 339 (2005) 338–344.

[21] B.H. Bielski, G.G. Shiue, S. Bajuk, Reduction of nitro blue tetrazolium by CO_2^- and O_2^- radicals, J. Phys. Chem. (United States) 84 (1980).

[22] J.M. Burns, W.J. Cooper, J.L. Ferry, D.W. King, B.P. DiMento, K. McNeill, C.J. Miller, W.L. Miller, B.M. Peake, S.A. Rusak, A.L. Rose, T.D. Waite, Methods for reactive oxygen species (ROS) detection in aqueous environments, Aquat. Sci. 74 (2012) 683–734.

[23] M.-T. Maurette, E. Oliveros, P.P. Infelta, K. Ramsteiner, A.M. Braun, Singlet oxygen and superoxide: experimental differentiation and analysis, Helv. Chim. Acta 66 (1983) 722–733.

[24] P. Fernández-Castro, M. Vallejo, M.F. San Román, I. Ortiz, Insight on the fundamentals of advanced oxidation processes. Role and review of the determination methods of reactive oxygen species, J. Chem. Technol. Biotechnol. 90 (2015) 796–820.

[25] L. Wang, M. Cao, Z. Ai, L. Zhang, Design of a highly efficient and wide pH electro-Fenton oxidation system with molecular oxygen activated by ferrous–tetrapolyphosphate complex, Environ. Sci. Technol. 49 (2015) 3032–3039.

[26] A.D. Bokare, W. Choi, Singlet-oxygen generation in alkaline periodate solution, Environ. Sci. Technol. 49 (2015) 14392–14400.

[27] J. He, X. Yang, B. Men, D. Wang, Interfacial mechanisms of heterogeneous Fenton reactions catalyzed by iron-based materials: a review, J. Environ. Sci. 39 (2016) 97–109.

[28] H.H. Jaffe, A reexamination of the Hammett equation, Chem. Rev 53 (1953) 191–261.

[29] O. Exner, The Hammett equation—the present position, in: N.B. Chapman, J. Shorter (Eds.), Advances in Linear Free Energy Relationships, Springer US, Boston, MA, 1972, pp. 1–69.

[30] C. Hansch, A. Leo, R. Taft, A survey of Hammett substituent constants and resonance and field parameters, Chem. Rev. 91 (1991) 165–195.

[31] L.K. Charkoudian, K.J. Franz, Fe(III)-coordination properties of neuromelanin components: 5,6-dihydroxyindole and 5,6-dihydroxyindole-2-carboxylic acid, Inorg. Chem. 45 (2006) 3657–3664.

[32] N.R. Perron, J.L. Brumaghim, A review of the antioxidant mechanisms of polyphenol compounds related to iron binding, Cell Biochem. Biophys. 53 (2009) 75–100.

[33] A. Avdeef, S.R. Sofen, T.L. Bregante, K.N. Raymond, Coordination chemistry of microbial iron transport compounds. 9. Stability constants for catechol models of enterobactin, J. Am. Chem. Soc. 100 (1978) 5362–5370.

[34] N.P. Slabbert, Ionisation of some flavanols and dihydroflavonols, Tetrahedron 33 (1977) 821–824.

[35] R. Pizer, L. Babcock, Mechanism of the complexation of boron acids with catechol and substituted catechols, Inorg. Chem. 16 (1977) 1677–1681.

[36] J.L. Beltrán, N. Sanli, G. Fonrodona, D. Barrón, G. Özkan, J. Barbosa, Spectrophotometric, potentiometric and chromatographic pKa values of polyphenolic acids in water and acetonitrile–water media, Anal. Chim. Acta 484 (2003) 253–264.

[37] V.M. Nurchi, T. Pivetta, J.I. Lachowicz, G. Crisponi, Effect of substituents on complex stability aimed at designing new iron(III) and aluminum(III) chelators, J. Inorg. Biochem. 103 (2009) 227–236.

[38] M.J. Hynes, M.n. O'Coinceanainn, The kinetics and mechanisms of reactions of iron (III) with caffeic acid, chlorogenic acid, sinapic acid, ferulic acid and naringin, J. Inorg. Biochem. 98 (2004) 1457–1464.

[39] V. Kristinová, R. Mozuraityte, I. Storrø, T. Rustad, Antioxidant activity of phenolic acids in lipid oxidation catalyzed by different prooxidants, J. Agric. Food Chem. 57 (2009) 10377–10385.

[40] R.C. Hider, B. Howlin, J.R. Miller, A.R. Mohd-Nor, J. Silver, Model compounds for microbial iron-transport compounds. Part IV. Further solution chemistry and Mössbauer studies on iron(II) and iron(III) catechol complexes, Inorg. Chim. Acta 80 (1983) 51–56.

[41] H. Powell, M. Taylor, Interactions of iron(II) and iron(III) with gallic acid and its homologues: a potentiometric and spectrophotometric study, Aust. J. Chem. 35 (1982) 739–756.

[42] D. Contreras, J. Freer, J. Rodríguez, Veratryl alcohol degradation by a catechol-driven Fenton reaction as lignin oxidation by brown-rot fungi model, Int, Biodeterior. Biodegrad. 57 (2006) 63–68.

[43] V. Melin, A. Henríquez, J. Freer, D. Contreras, Reactivity of catecholamine-driven Fenton reaction and its relationships with iron(III) speciation, Redox Rep. 20 (2015) 89–96.

[44] L. Wang, Y. Yao, L. Sun, Y. Mao, W. Lu, S. Huang, W. Chen, Rapid removal of dyes under visible irradiation over activated carbon fibers supported Fe(III)–citrate at

neutral pH, Sep. Purif. Technol. 122 (2014) 449–455.

[45] Y. Yao, Y. Mao, B. Zheng, Z. Huang, W. Lu, W. Chen, Anchored iron ligands as an efficient Fenton-like catalyst for removal of dye pollutants at neutral pH, Ind. Eng. Chem. Res. 53 (2014) 8376–8384.

[46] E. Finkelstein, G.M. Rosen, E.J. Rauckman, Spin trapping. Kinetics of the reaction of superoxide and hydroxyl radicals with nitrones, J. Am. Chem. Soc. 102 (1980) 4994–4999.

[47] D. Contreras, J. Rodríguez, J. Freer, B. Schwederski, W. Kaim, Enhanced hydroxyl radical production by dihydroxybenzene-driven Fenton reactions: implications for wood biodegradation, JBIC J. Biol. Inorg. Chem. 12 (2007) 1055–1061.

[48] Y. Wang, H. Xia, K. Sun, S. Wu, W. Lu, J. Xu, N. Li, K. Pei, Z. Zhu, W. Chen, Insights into the generation of high-valent copper-oxo species in ligand-modulated catalytic system for oxidizing organic pollutants, Chem. Eng. J. 304 (2016) 1000–1008.

[49] P.K. Malik, Oxidation of safranine T in aqueous solution using Fenton's reagent: involvement of an Fe(III) chelate in the catalytic hydrogen peroxide oxidation of safranine T, J. Phys. Chem. A 108 (2004) 2675–2681.